The results of measurements within the bracket of Reynolds number from 10^4 to 195000 can be expressed by equation

$$Nu = 0{\cdot}33\,(Gr + Re^2)^{0{\cdot}25}. \quad (4)$$

The effect of free convection was allowed for by Grashof number (as in [4]), the influence of which on the value of heat-transfer coefficient at the local Reynolds numbers greater than 3×10^4 did not exceed 6 per cent. The small deviation of the measurement results from the theoretical values for low Reynolds numbers, may have resulted from a some difference between a theoretical and an experimental flow models due to a final diameter of the test disk. The table below contains a comparison of the results of some experiments with an analitycal prediction. The results of measurements by Cobb and Saunders [5], as well as those by Richardson and Saunders [4], obtained on the same stand are probably too high due to disturbing influence of the shaft and stand elements.

Table 1. Comparison of experimental results with a theoretical solution (for $Pr = 0{\cdot}71$)

Author	$\dfrac{Nu}{(Gr+Re^2)^{0{\cdot}25} f(Pr = 0{\cdot}71)}$
Experiments of:	
Richardson and Saunders [4]	0·40
Cobb and Saunders [5]	0·36
Kreith, Taylor and Chong [6]	0·34
McComas and Hartnett [3]	0·33
Authors of this paper	0·33
Analytical solution of:	
Hartnett [7]	0·33

Within the range of Reynolds number from 195000 to 250000 there is a fast increase of local heat-transfer coefficients. The limits of this region overlap quite well with the points of stability loss of the laminar boundary layer and the beginning of turbulent boundary layer on the rotating disk, as determined by Gregory and Walker [8].

The local heat transfer in the transition region can be expressed by following equation*

$$Nu = 10 \times 10^{-20}\, Re^4. \quad (5)$$

The measurement results worked out within the range of Reynolds numbers from 250000 to 670000 at the constant radius $R = 185$ mm can be expressed by the equation*

$$Nu = 0{\cdot}0188\, Re^{0{\cdot}8}. \quad (6)$$

An average Nusselt number $\overline{Nu} = Nu/1{\cdot}3 = 0{\cdot}0145\, Re^{0{\cdot}8}$ is 3·7 per cent lower than those obtained by Cobb and Saunders [5].

REFERENCES

1. F. Kreith, Convection heat transfer in rotating systems, in *Advances in Heat Transfer*, Vol. 5, pp. 129–251. Academic Press, New York (1968).
2. L. A. Dorfman, Heat and mass transfer near rotating surfaces (Review), *J. Engng Phys.* **22**(2), 350–362 (1972).
3. S. T. McComas and J. P. Hartnett, Temperature profiles and heat transfer associated with a single disk rotating in still air, in *Proc. Fourth Int Heat Transfer Conference*, Vol. 3, FC 7.7. Versailles (1970).
4. P. D. Richardson and O. A. Saunders, Studies of flow and heat transfer associated with a rotating disk, *J. Mech. Engng Sci.* **5**(4), 336–342 (1963).
5. E. C. Cobb and O. A. Saunders, Heat transfer from a rotating disk, *Proc R. Soc.* **A236**(1206), 343–351 (1956).
6. F. Kreith, J. H. Taylor and J. P. Chong, Heat and mass transfer from a rotating disk, *J. Heat Transfer* **81**, 95–105 (1959).
7. J. P. Hartnett, Heat transfer from a nonisothermal disk rotating in still air, *J. Appl. Mech.* **26**, 672–673 (1959).
8. N. Gregory, J. T. Stuart and W. S. Walker, On the stability of three-dimensional boundary layers with application to the flow due to a rotating disk, *Phil. Trans. R. Soc.* **A248**(943), 155–199 (1955).

*The effect of the finite width of the *h*-calorimeter was duly allowed for, i.e. lowering of the measured values by 1·6 per cent in the transition region, and by 0·7 per cent in the turbulent region.

Int. J. Heat Mass Transfer. Vol. 18, pp. 170–174. Pergamon Press 1975. Printed in Great Britain

EXACT SOLUTIONS FOR MULTI-DIMENSIONAL RADIATIVE TRANSFER IN NON-ISOTHERMAL SPHERICAL MEDIA

PING CHENG* and SHYAM S. DUA†
Department of Mechanical Engineering, University of Hawaii, Honolulu, Hawaii

(*Received* 22 *October* 1973 *and in revised form* 6 *May* 1974)

NOMENCLATURE

Bu, Bouguer number or optical thickness, $Bu = \alpha_a L$;
I, specific radiation intensity;
J, dimensionless average radiation intensity, $J \equiv M/4\sigma T_r^4$;
L, reference length;
l_Θ, l_Φ, l_r, direction-cosines;
M, space integrated radiation intensity, $M \equiv \int I\, d\Omega$;
Q_θ, Q_Φ, Q_r, normalized radiation heat flux, $Q = q/\sigma T_r^4$;
q_θ, q_Φ, q_r, radiation heat flux in θ, Φ and r-direction;
R, position vector in the global spherical coordinate system;

*Professor.
†Graduate Student.

r, one of the global spherical coordinates;
s_1, s_2, s_3, coordinates defined by equation (4);
T_g, temperature of the medium;
T_r, reference temperature;
α_a, absorption coefficient;
θ, one of the local spherical coordinates;
θ_1, $\theta_1 \equiv \sin^{-1}(r_i/r)$;
Θ, one of the global spherical coordinates;
σ, Stefan–Boltzmann constant;
Φ, one of the global spherical coordinates;
ϕ, one of the local spherical coordinates.

Superscripts

*, quantities at the wall;
i, quantities associated with inner sphere;
o, quantities associated with outer sphere.

Subscripts

i, quantities associated with inner sphere;
o, quantities associated with outer sphere;
g, radiative quantities resulting from medium emission;
w, radiative quantities resulting from wall emission.

INTRODUCTION

In spite of the fact that the analytical expression of radiative heat flux in terms of temperature distribution for spherically symmetric configurations has been known for quite some time [1–3], the generalization of this expression for a three-dimensional temperature field has never been achieved. Recently, however, Bohachevsky and Kostoff [4] have succeeded in devising elaborate numerical procedures, based on geometric considerations, for the exact computation of multi-dimensional radiative transfer in spherical media with an axisymmetric temperature field. In this paper, closed form exact solutions are obtained for multi-dimensional radiative transfer in a non-isothermal medium between concentric spheres as well as inside and outside of a sphere. The approach adopted in this paper is an extension of previous work by Cheng *et al.* [5, 6], on the exact solutions of the radiative transport equation in rectangular and cylindrical coordinate systems.

RADIATIVE TRANSFER IN A THREE-DIMENSIONAL TEMPERATURE FIELD

For a three-dimensional temperature field in a spherical configuration where the temperature is given by $T_g(r, \Theta, \phi)$, the radiation-transport equation for a grey gas in thermodynamical equilibrium is [7]

$$\left[\cos\theta\frac{\partial}{\partial r}+\frac{\sin\theta\cos\phi}{r}\frac{\partial}{\partial\Theta}+\frac{\sin\theta\sin\phi}{r\sin\Theta}\frac{\partial}{\partial\Phi}-\frac{\sin\theta}{r}\frac{\partial}{\partial\theta}-\frac{\sin\theta\sin\phi}{r\tan\Theta}\frac{\partial}{\partial\phi}+\alpha_a\right]I=\frac{\alpha_a\sigma T_g^4}{\pi}(r,\Theta,\phi), \quad (1)$$

where r, Θ, Φ are the global spherical coordinates and θ, ϕ are the local spherical coordinates (see Fig. 1); α_a and σ are the absorption coefficient and the Stefan–Boltzmann constant, respectively. I is the specific radiation intensity which is a function of position vector $\bar{R}$ (where $\bar{R} = r\bar{e}_r$) and directional vector $\bar{e}_\Omega$ given by

$$\bar{e}_\Omega = \sin\theta\cos\phi\,\bar{e}_\Theta + \sin\theta\sin\phi\,\bar{e}_\Phi + \cos\theta\,\bar{e}_r, \quad (2)$$

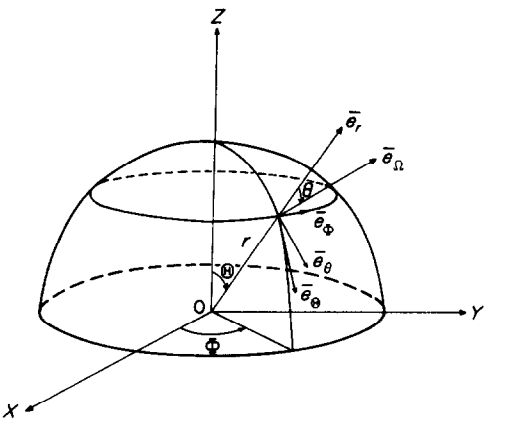

FIG. 1. Spherical coordinate system.

where $\bar{e}_r$, $\bar{e}_\Theta$ and $\bar{e}_\Phi$ are unit vectors of the global spherical coordinates.

If an isothermal black wall at a temperature T_w exists in the radiation field, the radiative boundary condition is given by

$$I(r^*, \Theta^*, \Phi^*, \theta^*, \phi^*) = \frac{\sigma T_w^4}{\pi}, \quad (3)$$

where r^*, Θ^*, Φ^* specify the position vector and θ^*, ϕ^* specify the direction vector, with the superscript "*" denoting quantities on the wall.

To obtain the formal solution of equation (1) with boundary condition (3) in spherical configurations we recast these equations in terms of the new independent variables $s_j (j = 1, 2, 3)$ with

$$s_1 \equiv \bar{R}.\bar{e}_\Omega, \quad s_2 \equiv \bar{R}.\bar{e}_\phi, \quad s_3 \equiv \bar{R}.\bar{e}_\theta, \quad (4)$$

where

$$\bar{e}_\phi = -\sin\phi\,\bar{e}_\Theta + \cos\phi\,\bar{e}_\Phi, \quad (5)$$

and

$$\bar{e}_\theta = \cos\theta\cos\phi\,\bar{e}_\Theta + \cos\theta\sin\phi\,\bar{e}_\Phi - \sin\theta\,\bar{e}_r,$$

which are the unit vectors of the local spherical coordinates. It follows from equations (4) and (5) that

$$s_1 = r\cos\theta, \quad s_2 = 0, \quad \text{and} \quad s_3 = -r\sin\theta. \quad (6)$$

If an isothermal black wall at a temperature T_w exists in the radiation field, the radiative boundary condition is given by

$$I(s_1, s_3, \theta, \phi) = \frac{\sigma T_w^4}{\pi}\exp[-\alpha_a(s_1 - s_1^*)] + \frac{\sigma}{\pi}\int_0^{s_1 - s_1^*} \alpha_a T_g^4(\tilde{s}_1', s_3, \theta, \phi) \times \exp[\alpha_a(\tilde{s}_1' - \tilde{s}_1)]\,d\tilde{s}_1', \quad (7)$$

where $\tilde{s}_1' = s_1' - s_1^*$, and $(s_1 - s_1^*)$ is the physical distance along s_1 from the field point (r, Θ, Φ) to that of the wall. In the subsequent discussion, it is convenient to refer to the first term in equation (7) as I_w and the second term as I_g, representing the contribution from wall emission as well as medium emission respectively.

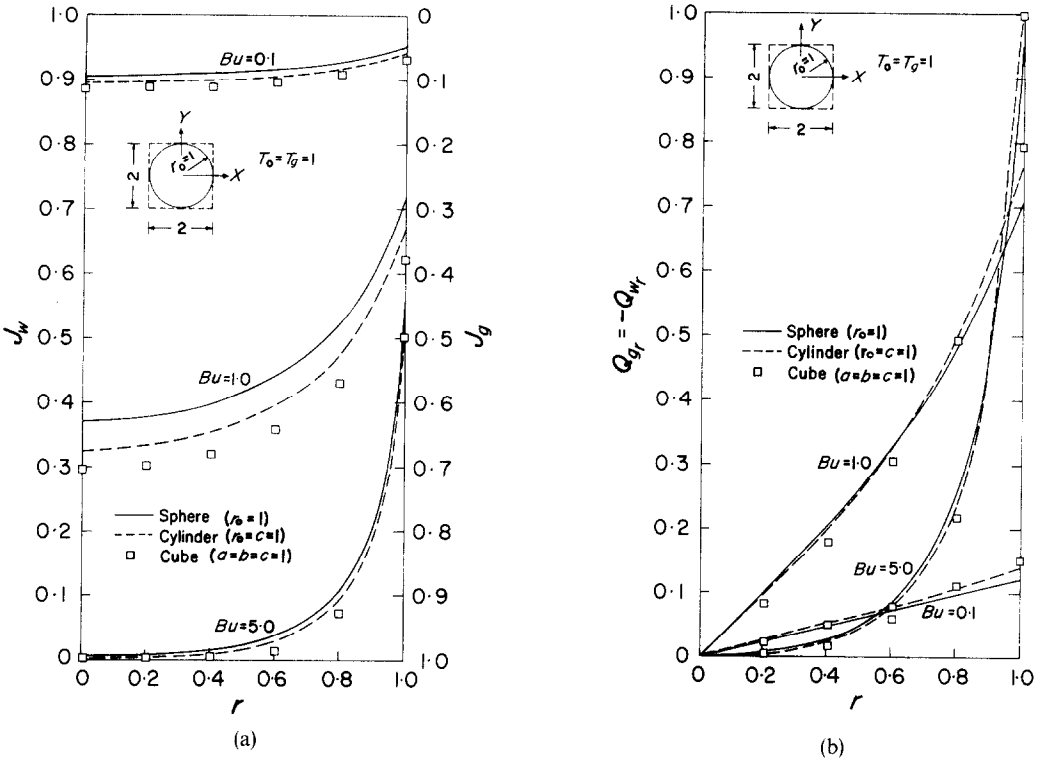

FIG. 2. Comparison of radiation fields inside an isothermal sphere (along r), an isothermal cylinder (along r at $z = 0$), and an isothermal cube (along x on $y = z = 0$).

It is worth mentioning, in passing, that from geometric consideration, we have $s_3 = s_3^*$ which, with the aid of equation (6), gives

$$\sin\theta^* = \frac{r}{r^*}\sin\theta. \tag{8}$$

Equation (8) will be useful to express the quantity $s_1 - s_1^*$ in equation (7) in terms of the spherical coordinates for various situations in subsequent discussion.

Emitting–absorbing medium between concentric spheres

Consider an emitting–absorbing medium with a prescribed temperature $T_g(r, \Theta, \Phi)$ between concentric spheres with radii r_i and r_o. If the temperatures of the black walls are T_i and T_0 respectively, the boundary conditions are given by

$$I(r_i, \Theta^*, \Phi^*, \theta^*, \phi^*) = \frac{\sigma T_i^4}{\pi}, \quad \text{for} \quad \bar{e}_\Omega \cdot \bar{e}_r^* \geqslant 0, \tag{9a}$$

$$I(r_o, \Theta^*, \Phi^*, \theta^*, \phi^*) = \frac{\sigma T_0^4}{\pi}, \quad \text{for} \quad \bar{e}_\Omega \cdot \bar{e}_r^* \leqslant 0. \tag{9b}$$

It follows from equation (2) that the condition $\bar{e}_\Omega \cdot \bar{e}_r^* \geqslant 0$ implies that $\cos\theta^* \geqslant 0$ and that the condition $\bar{e}_\Omega \cdot \bar{e}_r^* \leqslant 0$ implies that $\cos\theta^* \leqslant 0$.

Imposing boundary condition (9a), we have $r^* = r_i$ and $\cos\theta^* \geqslant 0$. It follows that

$$s_1 - s_1^* = r\cos\theta - \sqrt{(r_i^2 - r^2\sin^2\theta)}, \tag{10a}$$

where we have made use of equations (6) and (8). Similarly, imposing boundary condition (9b), we have

$$s_1 - s_1^* = r\cos\theta + \sqrt{(r_o^2 - r^2\sin^2\theta)}, \tag{10b}$$

where we have made use of equations (6), (8) and the condition $\cos\theta^* \leqslant 0$.

It follows from equation (7) and equations (10) that

$$I_w^{(i)} = \frac{\sigma T_i^4}{\pi}\exp\left[-\alpha_a(r\cos\theta - \sqrt{(r_i^2 - r^2\sin^2\theta)}\right], \tag{11a}$$

$$I_g^{(i)} = \frac{\sigma}{\pi}\int_0^{r\cos\theta - \sqrt{(r_i^2 - r^2\sin^2\theta)}} \alpha_a T_g^4(\tilde{s}_1', s_3, \theta, \phi) \times \exp\left[\alpha_a(\tilde{s}_1' - \tilde{s}_1)\right] d\tilde{s}_1' \tag{11b}$$

and

$$I_w^{(0)} = \frac{\sigma T_o^4}{\pi}\exp\left[-\alpha_a(r\cos\theta + \sqrt{(r_o^2 - r^2\sin^2\theta)})\right], \tag{11c}$$

$$I_g^{(0)} = \frac{\sigma}{\pi}\int^{r\cos\theta + \sqrt{(r_o^2 - r^2\sin^2\theta)}} \alpha_a T_g^4(\tilde{s}_1', s_3, \theta, \phi) \times \exp\left[\alpha_a(\tilde{s}_1' - \tilde{s}_1)\right] d\tilde{s}_1'. \tag{11d}$$

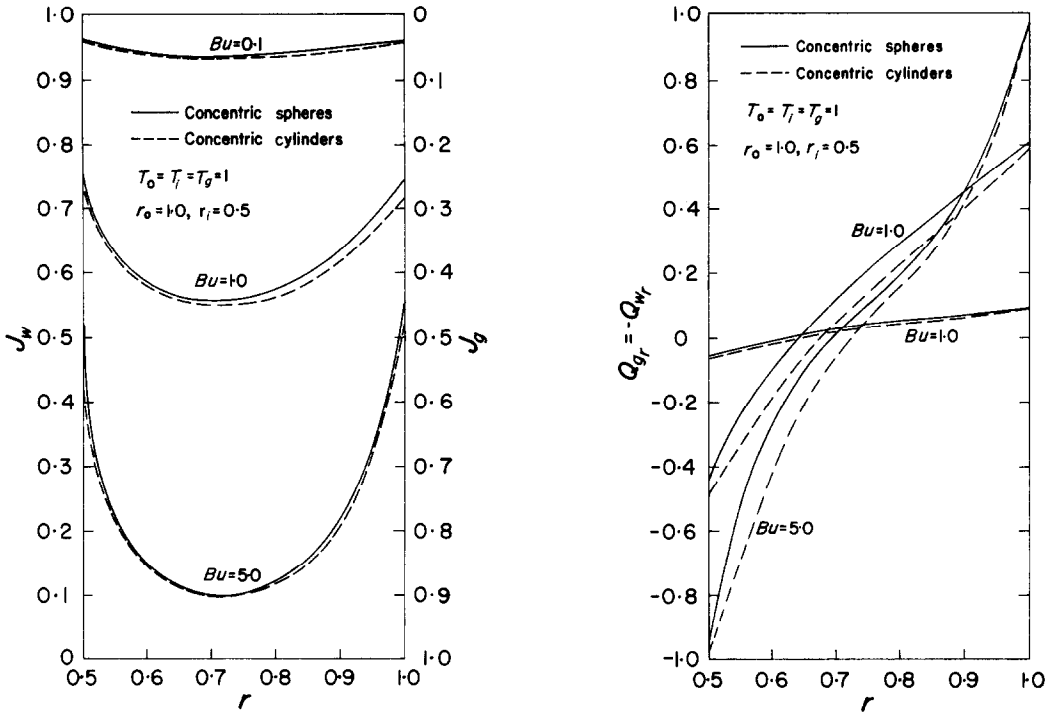

FIG. 3. Comparison of radiation fields between two concentric spheres (along r) and two concentric cylinders (along r at $z = 0$).

Consequently, the radiative quantities resulting from medium emission are given by

$$\begin{Bmatrix} M_g(r,\Theta,\Phi) \\ q_{g\Theta}(r,\Theta,\Phi) \\ q_{g\Phi}(r,\Theta,\Phi) \\ q_{gr}(r,\Theta,\Phi) \end{Bmatrix} = \int_{\phi=0}^{2\pi}\int_{\theta=0}^{\theta_1} I_g^{(i)} \begin{Bmatrix} 1 \\ l_\Theta \\ l_\Phi \\ l_r \end{Bmatrix} d\Omega + \int_{\phi=0}^{2\pi}\int_{\theta_1}^{2\pi} I_g^{(0)} \begin{Bmatrix} 1 \\ l_\Theta \\ l_\Phi \\ l_r \end{Bmatrix} d\Omega, \quad (r_i \leqslant r \leqslant r_o) \quad (12)$$

where $l_\theta \equiv \sin\theta\cos\phi$, $l_\Phi = \sin\theta\sin\phi$, $l_r \equiv \cos\theta$, and $\theta_1 \equiv \sin^{-1}(r_i/r)$. The radiative quantities resulting from wall emission are also given by equation (12) with the subscript g replaced by w.

Emitting–absorbing medium inside and outside of a sphere

The exact solutions for multi-dimensional radiative transfer in an emitting–absorbing medium with three-dimensional temperature distribution $T_g(r,\Theta,\Phi)$ inside and outside of a sphere can be obtained from equation (12) with suitable modifications. For example, for the case of an emitting–absorbing medium outside of a sphere with radius r_i, the radiative quantities are given by equations (12), (11c) and (11d) with $r_o \to \infty$ and $T_0 = 0$. For the case of an emitting–absorbing medium inside a sphere with radius r_o, the radiative quantities are given by dropping the first term in equation (12). This can be obtained formally by letting $r_i \to 0$ to give $\theta_1 = 0$ and consequently the first integral in equation (12) vanishes.

NUMERICAL RESULTS AND DISCUSSION

Computations were carried out for radiative transfer in an isothermal emitting-medium inside a sphere and between concentric spheres with isothermal walls. Numerical results in terms of dimensionless quantities J, Q, $\tilde{T}$, $\tilde{r}$, and Bu (where $J \equiv M/4\sigma T_r^4$, $Q \equiv q/\sigma T_r^4$, $\tilde{T} = T/T_r$, $\tilde{r} = r/L$, $Bu = \alpha_a L$ with T_r and L being the reference temperature and length respectively) are presented in Figs. 2 and 3. For the convenience of subsequent discussion, the superscript "~" will be omitted.

Figure 2(a) shows the variation of J_w and J_g along r inside an isothermal sphere with $T_w = T_g = r_o = 1$. It should be noted that $J_w = 1 - J_g$ when $T_w = T_g = 1$, and therefore J_w and J_g can be plotted in the same figure. Figure 2 also shows the comparison of the corresponding quantities along r on $z = 0$ inside a finite cylinder with $r = c = T_g = T_w = 1$, as well as along $(x, 0, 0)$ inside a cube* with $a = b = c = 1 = T_g = T_w = 1$. It is shown that for a specific value of Bu and at the same location, the value of J_w is largest for a sphere and smallest for a cube. This is because for the same point in the radiation field, the distance from the point under consideration to the wall is smallest for a sphere and largest for a cube. Consequently, wall emission has a greater effect for the case of a sphere than that of a cube. The effect of geometries on Q_{wr} and Q_{gr} is relatively small, as is shown in Fig. 2(b). The relative magnitudes of radiative heat flux inside a sphere, a cylinder, and a cube depends on the

*The horizontal scales in Figs. 2–5 of [5] were erroneously plotted. Instead of from 0 to 1, the horizontal scale should be from 0 to 0·5. In other words, the numerical results presented in [5] are for rectangles and cubes with unit length for each side.

values of Bu as well as the particular location under consideration.

The radiation field along r in an isothermal medium between isothermal concentric spheres ($r_i = 0{\cdot}5$, $r_o = 1{\cdot}0$, $T_g = T_0 = T_i = 1$) is shown in Figs. 3(a) and 3(b). In these figures, comparison is also made with the radiation field inside two finite isothermal concentric cylinders ($r_i = 0{\cdot}5$, $r_o = c = 1$, $T_g = T_0 = T_i = 1$) along r on the mid-plane $z = 0$, which were obtained previously [6]. As would be expected, the radiation fields under comparison exhibit similar behavior. The magnitudes of J_w and Q_{wr}, however, are higher for a concentric sphere than that of a finite concentric cylinder.

REFERENCES

1. E. M. Sparrow, C. M. Vsiskin and H. A. Hubbard, radiation heat transfer in a spherical enclosure containing a participating, heat generating gas, *J. Heat Transfer* **83**, 199–206 (1961).
2. I. L. Rhyming, Radiative transfer between two concentric spheres separating by an absorbing and emitting gas, *Int. J. Heat Mass Transfer* **9**, 315–323 (1966).
3. R. Viskanta and P. S. Lass, Transient cooling of a spherical mass of high-temperature gas by thermal radiation, *J. Appl. Mech.* **32**, 740–746 (1965).
4. I. O. Bohachevsky and R. N. Kostoff, Supersonic flow over convex and concave shapes with radiation and ablation effects, Bellcomm TM-71-1013-5 (1971).
5. P. Cheng, Exact solutions and differential approximation for multi-dimensional radiative transfer in cartesian coordinate configuration, *Progress in Astronautics and Aeronautics*, Vol. 31, *Thermal Control and Radiation*, pp. 269–308. Edited by C. L. Tien: The MIT Press, Cambridge, Mass. (1972).
6. S. S. Dua and P. Cheng, Multi-dimensional radiative transfer in non-isothermal cylindrical media with non-isothermal bounding walls, *Int. J. Heat Mass Transfer*. To be published.
7. A. Vesugi and J. Tsujita, Diffuse reflection of a searchlight beam by slab, cylindrical, and spherical media, *Publs Astr. Soc. Japan* **21**, 370–383 (1969).